Measurement report: $PM_{2.5}$-bound nitrated aromatic compounds in Xi'an, Northwest China: Seasonal variations and contributions to optical properties of brown carbon

Wei Yuan[1,6], Ru-Jin Huang[1,2], Lu Yang[1], Ting Wang[1,6], Jing Duan[1,6], Jie Guo[1], Haiyan Ni[1,7], Yang Chen[3], Qi Chen[4], Yongjie Li[5], Ulrike Dusek[7], Colin O'Dowd[8], Thorsten Hoffmann[9]

[1]State Key Laboratory of Loess and Quaternary Geology, Center for Excellence in Quaternary Science and Global Change, Key Laboratory of Aerosol Chemistry & Physics, Institute of Earth Environment, Chinese Academy of Sciences, Xi'an 710061, China

[2]Institute of Global Environmental Change, Xi'an Jiaotong University, Xi'an 710049, China

[3]Chongqing Institute of Green and Intelligent Technology, Chinese Academy of Sciences, Chongqing 400714, China

[4]State Key Joint Laboratory of Environmental Simulation and Pollution Control, College of Environmental Sciences and Engineering, Peking University, Beijing 100871, China

[5]Department of Civil and Environmental Engineering, Faculty of Science and Technology, University of Macau, Taipa, Macau SAR 999078, China

[6]University of Chinese Academy of Sciences, Beijing 100049, China

[7]Centre for Isotope Research (CIO), Energy and Sustainability Research Institute Groningen (ESRIG), University of Groningen, 9747 AG, The Netherlands

[8]School of Physics and Centre for Climate and Air Pollution Studies, Ryan Institute, National University of Ireland Galway, University Road, Galway H91CF50, Ireland

[9]Institute of Inorganic and Analytical Chemistry, Johannes Gutenberg University Mainz, Duesbergweg 10−14, 55128 Mainz, Germany

Correspondence to: Ru-Jin Huang (rujin.huang@ieecas.cn)

Abstract

Nitrated aromatic compounds (NACs) are a group of key chromophores for brown carbon aerosol (light absorbing organic carbon, i.e., BrC), which affects radiative forcing. The chemical composition and sources of NACs and their contributions to BrC absorption, however, are still not well understood. In this study, $PM_{2.5}$-bound NACs in Xi'an, Northwest China, were investigated for 112 daily $PM_{2.5}$ filter samples from 2015 to 2016. Both the total concentrations and contributions from individual species of NACs show distinct seasonal variations. The seasonally averaged concentrations of NACs are 2.1 (spring), 1.1 (summer), 12.9 (fall), and 56 ng m^{-3} (winter). Thereinto, 4-nitrophenol is the major NAC component in spring (58%). The concentrations of 5-nitrosalicylic acid and 4-nitrophenol dominate in summer (70%), and the concentrations of 4-nitrocatechol and 4-nitrophenol dominate in fall (58%) and winter (55%). The NAC species show different seasonal patterns in concentrations, indicating differences in emissions and formation pathways. Source apportionment results using positive matrix factorization (PMF) further show large seasonal differences in the sources of NACs. Specifically, in summer, NACs were highly influenced by secondary formation and vehicle emissions (~80%), while in winter, biomass burning and coal combustion contributed the most (~75%). Furthermore, the light absorption contributions of NACs to BrC are wavelength dependent and vary greatly by season, with maximum contributions at ~330 nm in winter and fall and ~320 nm in summer and spring. The differences in the contribution to light absorption are associated with the higher mass fractions of 4-nitrocatechol (λ_{max}=345 nm) and 4-nitrophenol (λ_{max}=310 nm) in fall and winter, 4-nitrophenol in spring, and 5-nitrosalicylic acid (λ_{max}=315 nm) and 4-nitrophenol in summer. The mean contributions of NACs to BrC light absorption at the wavelength of 365 nm in different seasons are 0.14% (spring), 0.09% (summer), 0.36% (fall) and 0.91% (winter), which are about 6-9 times higher than their mass fractional contributions of carbon in total organic carbon. Our results indicate that the composition and sources of NACs have profound impacts on the BrC light absorption.

1 Introduction

Brown carbon (BrC) aerosol has received growing attention over the past years, because it can affect the atmospheric radiation balance and air quality through absorption of solar radiation in the near ultraviolet and visible range (Feng et al., 2013; Laskin et al., 2015; Zhang et al., 2017; Ma et al., 2018; Ma et al., 2019). Nitrated aromatic compounds (NACs) belong to a major group of BrC chromophores. They are ubiquitous in the atmosphere and have been detected in cloud water (Desyaterik et al., 2013), rainwater (Schummer et al., 2009), fog water (Richartz et al., 1990), snow water (Vanni et al., 2001), as well as in gas and particle phases (Cecinato et al., 2005; Zhang et al., 2013; Chow et al., 2015; Al-Naiema and Stone, 2017). Field studies have shown that ~4% of BrC light absorption at 370 nm is contributed by the measured NACs (Zhang et al., 2013; Mohr et al., 2013; Teich et al., 2017; X. Li et al., 2020). For example, Zhang et al. (2013) estimated the contribution of NACs to BrC light absorption of ~4% in the Los Angeles Basin. Mohr et al. (2013) calculated the contribution of NACs to BrC light absorption of about 4% in Detling, United Kingdom. Teich et al. (2017) investigated the contribution of NACs to BrC light absorption during six campaigns of 0.02-4.41% for acidic conditions and 0.02-9.86% for alkaline conditions. X. Li et al. (2020) estimated the contribution of NACs to BrC light absorption in Beijing of 0.28-3.44% in fall and 1.03-6.49% in winter. In addition, with molecular structures commonly containing nitro (-NO_2) and hydroxyl (-OH) functional groups on the aromatic ring, NACs are harmful to human health (Taneda et al., 2004). For example, NACs can interact with DNA and cause mutagenesis (Purohit and Basu, 2000; Ju and Parales, 2010). NACs can also damage cells, resulting in cell degeneration and canceration (Kovacic and Somanathan, 2014). There is also evidence that NACs affect plant growth and contributed to forest decline (Hinkel et al., 1989; Natangelo et al., 1999). The significant role of NACs in the atmosphere and their adverse effects on ecosystems call for studies to investigate their sources and characteristics.

NACs in atmospheric aerosol can be derived from primary emissions, including biomass burning (Wang et al., 2017; Teich et al., 2017; Lin et al., 2018), coal combustion (Olson et al., 2015; Lu et al., 2019a), and vehicle exhausts (Taneda et al., 2004; Inomata et al., 2013; Perrone et al., 2014; Lu et al., 2019b). The emission factors of NACs from biomass burning can be over 10 mg kg^{-1} (Wang et al., 2017), which makes them good tracers of biomass

burning organic aerosol (BBOA) (Hoffmann et al., 2007; Iinuma et al., 2010). Lu et al. (2019a) determined that the emission factors of fine particulate NACs for residential coal combustion were 0.2-10.1 mg kg^{-1} and the total NAC emission from residential coal burning was nearly 200 Mg in China in 2016. NACs from vehicle exhaust also have been detected, with emission factors of up to 26.7 μg km^{-1} (Lu et al., 2019b). Secondary formation from various atmospheric reactions is also an important source of NACs. For example, photochemical oxidation of benzene, toluene (Wang et al., 2019), and *m*-cresol (Iinuma et al., 2010) can form certain NACs. NACs can also form in aerosol or cloud water through aqueous-phase reactions (Vione et al., 2001, 2005), for example, photonitration of guaiacol in the aqueous phase (Kitanovski et al., 2014). However, little is known about the importance of primary versus secondary sources for particle-bound NACs because speciation of NACs and quantification of their sources are still very limited so far.

Speciation of particle-bound NACs was mostly performed in Europe (Cecinato et al., 2005; Iinuma et al., 2010; Delhomme et al., 2010; Mohr et al., 2013; Kahnt et al., 2013), and is still very scarce in Asia (Chow et al., 2015; Wang et al., 2018; Ikemori et al., 2019). In general, the average concentrations of measured NACs vary from less than one to dozens of ng m^{-3} in different seasons and regions. As far as we know, only one study has quantified the sources of NACs with a positive matrix factorization (PMF) receptor model (Wang et al., 2018). Here, we carried out chemical analyses together with light absorption for $PM_{2.5}$ samples collected in Xi'an to: 1) investigate the seasonal variations in the concentration of NACs and contributions of individual species; 2) quantify the sources of NACs in different seasons based on the PMF model; and 3) evaluate the optical properties of NACs and their contributions to BrC light absorption.

2 Experiments and methods

2.1 Aerosol sampling

24 h-integrated $PM_{2.5}$ samples were collected in four seasons from November 2015 to November 2016 (i.e., from 30 November to 31 December 2015 for winter; 19 April to 19 May 2016 for spring; 1 to 31 July 2016 for summer; and 9 October to 15 November 2016 for fall)

in the campus of the Institute of Earth Environment, Chinese Academy of Sciences (IEECAS, 34.22°N, 109.01°E) in Xi'an, China. The sampling site is an urban background site surrounded by residential areas and has no obvious industrial activities. A total of 112 samples were collected on pre-baked (780 °C, 3 h) quartz-fiber filters (20.3 × 25.4 cm, Whatman, QM-A, Clifton, NJ, USA) by a Hi-Vol $PM_{2.5}$ sampler (Tisch, Cleveland, OH) operating at 1.05 m^3 min^{-1}. The filter samples were stored at -20 ◦C until laboratory analysis.

2.2 Chemical analysis

The concentration of organic carbon (OC) was measured by a Thermal/Optical Carbon Analyzer (DRI, Model 2001, Atmoslytic Inc., Calabasas, CA, USA) with the IMPROVE-A protocol (Chow et al., 2011). Ten NACs and 19 organic markers (see Table S1) were quantified by a gas chromatograph-mass spectrometer (GC-MS) using a well-established approach (e.g., Wang et al., 2006; Al-Naiema and Stone, 2017) and the details are described in Yuan et al. (2020). At least one blank filter sample was analyzed for every ten ambient samples. Baseline separation with symmetrical peak shapes was achieved for the measured NACs (Fig. 1). The linear ranges, instrument detection limit (IDL), instrument quantitation limit (IQL), extraction efficiency, and regression coefficients for the measured NACs are shown in Table S2. The response of calibration curves for the NACs was linear ($R^2 \geq 0.995$) from 10 to 5000 μg L^{-1}. The IDL ranged from 2 μg L^{-1} to 20 μg L^{-1} except for 5-nitrosalicylic acid (53 μg L^{-1}). The IQL ranged from below 10 μg L^{-1} to 70 μg L^{-1} except for 5-nitrosalicylic acid (> 100 μg L^{-1}). The IDL and IQL are comparable to those in Al-Naiema and Stone (2017) (2.7-14.9 μg L^{-1} for IDL and 8.8-50 μg L^{-1} for IQL) and are sufficient for the quantification of our samples.

2.3 Light absorption of NACs

A UV-Vis spectrophotometer equipped with a Liquid Waveguide Capillary Cell (LWCC-3100, World Precision Instrument, Sarasota, FL, USA) was used to measure the light absorption of methanol-soluble BrC and NAC standards, following the method established by Hecobian et al. (2010). The absorption coefficient (Abs_λ: M m^{-1}) can be obtained from the measured absorption data by equation (1):

$$Abs_{\lambda} = (A_{\lambda} - A_{700}) \frac{V_l}{V_a \times L} \ln(10) \quad (1)$$

where A_{700} is the absorption at 700 nm used to correct for baseline drift, V_l is the volume of methanol used for extracting the filter, V_a is the volume of sampled air, L is 0.94 m for the optical path length used in the LWCC, and ln(10) is used to convert the absorption coefficient from log base-10 to natural logarithm.

The mass absorption efficiency (MAE: $m^2\ g^{-1}$) of NAC standards in the methanol solvent at wavelength of λ can be calculated as Laskin et al. (2015):

$$MAE_{NAC,\lambda} = \frac{A_{\lambda} - A_{700}}{L \times C} \ln(10) \quad (2)$$

where C ($\mu g\ mL^{-1}$) is the concentration of the NAC standards in the methanol solvent.

The light absorption contribution of NACs to BrC at wavelength of λ ($Cont_{NAC/BrC,\lambda}$) can be obtained using equation (3).

$$Cont_{NAC/BrC,\lambda} = \frac{MAE_{NAC,\lambda} \times C_{NAC}}{Abs_{BrC,\lambda}} \quad (3)$$

where the C_{NAC} ($\mu g\ m^{-3}$) is the atmospheric concentration of NACs and the $Abs_{BrC,\lambda}$ is the Abs of BrC at wavelength of λ.

2.4 Source apportionment

The sources of the NACs were resolved by the PMF receptor model, which was performed by the multilinear engine (ME-2; Paatero, 1997) through the Source Finder (SoFi) interface encoded in Igor Wavemetrics (Canonaco et al., 2013). The input species include five to ten NACs (as the number of NACs detected varies among seasons) and nineteen additional organic tracer species (see Table S1), with uncertainties (RSD) < 10%. These include phthalic acid for secondary formation, picene for coal combustion, hopanes for vehicle emission, fluoranthene, pyrene, chrysene, benzo(a)pyrene, benzo(a)anthracene, benzo(k)fluoranthene, benzo(b)fluoranthene, benzo(ghi)perylene, and indeno[1,2,3-cd]pyrene for combustion emission, and vanillin, vanillic acid, syringyl acetone, and levoglucosan for biomass burning. To separate the source profiles clearly, the contribution of those markers unrelated to a certain source was set to 0 in the respective source profile (see Table S3).

To better understand the source origins of the NACs, air mass origins during the sampling period were derived from backward-trajectory analysis. This method was used in

trajectory clustering based on the GIS-based software-TrajStat (Wang et al., 2009). The archived meteorological data was obtained from the National Center for Environmental Prediction's Global Data Assimilation System (GDAS). According to the lifetimes of the different secondary species (Wojcik and Chang, 1997; Chow et al., 2015), in this study, 72-h backward trajectories terminated at a height of 500 m above ground level were calculated during the study period. The trajectories were calculated every 12 h with starting times at 09:00 and 21:00 local time.

3 Results and discussion

3.1 Seasonal variations of NAC composition

The concentrations of the NACs show clear seasonal differences, with the highest mean values in winter, followed by fall, spring, and summer (see Fig. 2). The concentration ranges of total NACs were 1.4-3.4 ng m^{-3} (spring), 0.1-3.8 ng m^{-3} (summer), 1.6-44 ng m^{-3} (fall), and 20-127 ng m^{-3} (winter). The average concentrations were 2.1 ± 0.6 ng m^{-3}, 1.1 ± 0.8 ng m^{-3}, 12.9 ± 11.6 ng m^{-3} and 56 ± 23 ng m^{-3}, respectively (see Table S4). Nitrophenols (4-nitrophenol, 2-methyl-4-nitrophenol, 3-methyl-4-nitrophenol, 2,6-dimethyl-4-nitrophenol) and nitrocatechols (4-nitrocatechol, 3-methyl-5-nitrocatechol, 4-methyl-5-nitrocatechol) show the highest concentrations in winter and the lowest in summer, while nitrosalicylic acids (3-nitrosalicylic acid, 5-nitrosalicylic acid) show the highest concentrations in winter and the lowest in spring. The average ratios between wintertime and summertime concentrations are a factor of about 40 for nitrophenols, 175 for nitrocatechols, and 21 for nitrosalicylic acids. The large seasonal differences in NAC concentrations might be due to the differences in sources, emission strength and atmospheric formation processes, as discussed below. Table 1 summarizes the NAC concentrations measured in this study together with those measured in Europe, the USA and other places in Asia. In general, the NAC concentrations in winter are higher than those in summer, and the observed concentrations of different species are higher in Asia than in Europe and the USA. The only exception is a study in Ljubljana, Slovenia, which shows that in winter nitrocatechol concentrations are higher than those in Asia, likely due to strong biomass burning activities (Kitanovski et al., 2012). The elevated concentrations

of NACs in Asia suggest that NACs may have a significant impact on regional climate and air quality in Asia due to their optical and chemical characteristics, as discussed below.

Among all measured NACs, 4-nitrophenol, 2-methyl-4-nitrophenol, 3-methyl-4-nitrophenol, 4-nitrocatechol and 5-nitrosalicylic acid were detected in four seasons, 3-methyl-5-nitrocatechol and 4-methyl-5-nitrocatechol in fall and winter, 2,6-dimethyl-4-nitrophenol, 3-nitrosalicylic acid and 4-nitro-1-naphthol only in winter, as shown in Fig. 3a. In general, 4-nitrophenol and 4-nitrocatechol had elevated concentrations in all seasons, which is consistent with other observations (Chow et al., 2015; Ikemori et al., 2019) and might be related to their larger emissions or formation and longer atmospheric lifetime than other NACs (Harrison et al., 2005; Chow et al., 2015; Finewax et al., 2018; Wang et al., 2019; Lu et al., 2019a). For example, Lu et al. (2019a) measured the emission of NACs from coal combustion and found that the emission factors of 4-nitrocatechol were about 1.5-6 times higher than those of other NACs. Wang et al. (2019) quantified the concentrations of 4-nitrophenol and 4-nitrocatechol formed under high NO_x and anthropogenic VOC conditions, and found that they are about 3-7 times higher than those of other NACs. The concentration of 2-methyl-4-nitrophenol was higher than that of 3-methyl-4-nitrophenol in all seasons, which is similar to previous studies (Kitanovski et al., 2012; Chow et al., 2015; Teich et al., 2017; Ikemori et al., 2019) and likely due to the efficient formation of 2-methyl-4-nitrophenol from photochemical oxidation of volatile organic compounds (VOCs) in the presence of NO_2 (Lin et al., 2015; Wang et al., 2019). It should be noted that the contribution of 5-nitrosalicylic acid (27%) to total NAC mass in summer is much higher than in other seasons (4%-13%), suggesting that 5-nitrosalicylic acid is mainly produced by secondary formation, for example, through nitration of salicylic acid (M. Li et al., 2020) and photochemical oxidation of toluene in the presence of NO_x (Jang and Kamens, 2001; Wang et al., 2018).

3.2 Sources of NACs

Correlation analysis was conducted among the NACs measured in this study (Table S5). The four nitrophenols were positively correlated with each other (r^2 = 0.52-0.98) and the three nitrocatechols were also highly correlated with each other (r^2 = 0.94-0.96), indicating that the

different nitrophenols and nitrocatechols might have similar sources or origins. Previous studies showed that 4-nitrophenol was mainly from primary emission of biomass burning (Wang et al., 2017), and 3-methyl-5-nitrocatechol and 4-methyl-5-nitrocatechol were identified as secondary products from biomass burning (Iinuma et al., 2010). Positive correlations were also observed between nitrophenols and nitrocatechols (r^2 = 0.59-0.90), suggesting that they were partly of similar sources or formation processes. For example, both nitrophenols and nitrocatechols can be emitted through biomass burning (Wang et al., 2017) and coal combustion (Lu et al., 2019a) and can be formed by photochemical oxidation of VOCs in the presence of NO_2 (Wang et al., 2019). However, for nitrosalicylic acids, the correlation between 3-nitrosalicylic acid and 5-nitrosalicylic acid was weak (r^2 = 0.29). This is because 5-nitrosalicylic acid is mainly from secondary formation by nitration of salicylic acids, while 3-nitrosalicylic acid is mainly from combustion emission (Wang et al., 2017; M. Li et al., 2020). The correlations of nitrosalicylic acids with nitrophenols (r^2 = 0.01-0.13) and with nitrocatechols (r^2 = 0.04-0.25) were also weak, suggesting that they may have different sources or formation processes. Nitrosalicylic acids were dominated by 5-nitrosalicylic acids, which are mainly from secondary formation (Andreozzi et al., 2006; Wang et al., 2018). On the other hand, nitrophenols and nitrocatechols were dominated by 4-nitrophenol and 4-nitrocatechol, respectively, which are mainly from primary emissions (Wang et al., 2017; Lu et al., 2019a).

To identify and quantify the sources of the NACs observed in Xi'an, the PMF model was employed and four major factors were resolved with uncertainties < 15%. The factor profiles are shown in Fig. S1. The first factor, vehicle emission, characterized by high levels of hopanes, shows large relative contributions to NACs in spring and summer. Direct traffic emissions of NACs have also been verified in laboratory studies (Tremp et al., 1993; Perrone et al., 2014). The second factor is considered to be coal combustion for residential heating and cooking, which is characterized by the higher loadings of picene, benzo(a)pyrene, benzo(b)fluoranthene, benzo(k)fluoranthene, indeno[1,2,3-cd]pyrene, and benzo(ghi)perylene. This factor accounted for ~40% of the NACs in winter. The emission of NACs from coal combustion for residential usage was reported by Lu et al. (2019a), which

showed emission factors of 0.2 to 10.1 mg kg^{-1}. It is worth noting that with the emission control of residential coal burning after 2017, the contribution feature of coal burning to NACs could be different. The third source is identified as secondary formation because of the highest level of phthalic acid and its highest contribution in summer. The formation of secondary NACs is also supported by both field and modeling studies (Harrison et al., 2005; Iinuma et al., 2010; Yuan et al., 2016). The last source factor, with high loadings of levoglucosan, vanillic acid, vanillin and syringyl acetone, was identified as biomass burning, which has higher contributions in fall and winter. The emission of NACs from biomass burning was reported by field studies, and was considered to be an important source of NACs (Mohr et al., 2013; Lin et al., 2016; Teich et al., 2017).

The source contributions for NACs in Xi'an are shown in Fig. 4, which shows obvious seasonal differences. In spring, vehicular emission (41%) was the main contributor to NACs. Secondary formation (26%) and biomass burning (20%) also contributed significantly. In summer, secondary formation had the highest contribution (45%), which was likely due to enhanced photochemical oxidation leading to the formation of NACs. Besides, vehicular emission also contributed significantly (34%) in summer. In fall, biomass burning (45%) contributed the most, while secondary formation (30%) and vehicular emission (23%) also had significant contributions. In winter, coal burning (39%) and biomass burning (36%) were the main contributors, which can be attributed to emissions from residential heating activities. It is worth noting that the absolute concentrations of NACs attributed by vehicle emission (see Table S6) were higher in winter than those in spring and summer, yet these differences of less than 20 times are not as significant as the differences (spring and summer vs. winter) for NACs attributed by other primary emissions (> 80 times for coal burning and > 40 for biomass burning). These results indicate that anthropogenic primary sources are the main contributors to NACs in Xi'an, suggesting that control of anthropogenic emissions (biomass burning and coal burning) is important for mitigating pollution of NACs in this region. Secondary formation also contributes significantly to NACs, especially in summer. Further comprehensive field studies are necessary for understanding the formation mechanisms of NACs under different atmospheric conditions.

3.3 Backward trajectory analysis of NACs

To reveal the source origins of the NACs, the concentrations of the NACs were grouped according to their trajectory clusters that represent different air mass origins, as shown in Fig. 5. In general, the air masses from local emissions (Cluster 1 in spring and fall and Cluster 2 in summer and winter), which showed the features of small-scale and short-distance air transport, caused significant increases in NAC concentrations. As for regional transport, the air masses from the neighboring Gansu province across Baoji city before arriving at Xi'an presented higher concentrations of NACs in fall and winter (Cluster 2 and Cluster 3, respectively). In addition, air masses from Xinjiang across Gansu caused increased concentrations of NACs in spring and summer (Cluster 2 and Cluster 1, respectively). A small proportion of air masses from the northwest (Cluster 3 in spring and Cluster 1 in winter), the south (Cluster 3 in summer) and the west (Cluster 3 in fall), which showed long or moderate transport patterns, are related to the lowest concentrations of NACs. This may be due to the long-distance transport or relatively clean air from those regions. In the same season, the source origins of air masses were different between clusters, thus causing the difference in concentrations of NACs. However, the composition of NACs was similar between clusters, which is comparable to the results of Chow et al. (2015).

3.4 Light absorption of NACs

The correlations between NAC concentration and $Abs_{BrC,365}$ for each season are shown in Fig. S2. The correlations are stronger in fall (r^2 = 0.68) and winter (r^2 = 0.63) compared to those in spring (r^2 = 0.15) and summer (r^2 = 0.40). These results indicate that NACs are important components of BrC chromophores in fall and winter.

Fig. 6 shows the contributions of NACs to BrC light absorption at wavelength from 300 to 500 nm ($Abs_{BrC,300-500}$) as well as the carbon mass contributions of NACs to OC. The contributions of NACs to $Abs_{BrC,300-500}$ are wavelength dependent and vary largely in different seasons. High contributions at wavelengths of 350-400 nm were observed in fall and winter, but the contributions in spring and summer were mainly at wavelengths shorter than 350 nm. These results may be due to the high proportion of nitrocatechols in fall and winter (see

discussion above), which have strong light absorption at wavelength above 350 nm (see Fig. S3). The seasonal average contributions of NACs to $Abs_{BrC,365}$ were highest in winter (0.91 ± 0.30%), followed by fall (0.36 ± 0.22%), spring (0.14 ± 0.04%), and summer (0.09 ± 0.06%) (see Table S4). These contributions are comparable to a previous study where eight NACs were measured (Teich et al., 2017). The contributions of NACs to $Abs_{BrC,365}$ in winter were about 10 times higher compared to those in summer, which could be due to the high emissions of NACs in winter. Alternatively, enhanced atmospheric oxidizing capacity in the summer can lead to enhanced formation of secondary NACs or the degradation/bleaching of certain NACs (Barsotti et al., 2017; Hems and Abbatt, 2018; Wang et al., 2019) which might eventually reduce the contributions in summer. The fractions of NACs to total OC also show obvious seasonal variation, with average contributions higher in winter (0.14 ± 0.05%) and fall (0.05 ± 0.02%) and lower in spring (0.02 ± 0.01%) and summer (0.01 ± 0.01%). The contributions of NACs to BrC light absorption at 365 nm are, however, 6-9 times larger than their carbon mass contributions to total OC. Our results echo previous studies that even small amounts of chromophores can have a non-negligible impact on the optical characteristics of BrC due to their disproportional absorption contributions (Mohr et al., 2013; Zhang et al., 2013; Teich et al., 2017; Xie et al., 2017).

The daily contributions of the individual NACs to light absorption of total NACs at wavelength of 300-500 nm are shown in Fig. 7. Similar to the concentration fractions in NACs, nitrocatechols were the main contributors in winter and fall with contributions of 38-65% and 18-62%, respectively. On the other hand, nitrophenols dominated in spring and summer with contributions of 61-96% and 27-100%, respectively. As for nitrophenols, 4-nitrophenol was the most important chromophore, followed by 2-methyl-4-nitrophenol, 3-methyl-4-nitrophenol, and 2,6-dimethyl-4-nitrophenol (only observed in winter). As for nitrocatechols, 4-nitrocatechol was the main contributor in all four seasons, while 3-methyl-5-nitrocatechol and 4-methyl-5-nitrocatechol also contributed significantly in fall and winter. For nitrosalicylic acids, 5-nitrosalicylic acid contributed in all four seasons but contributed the most in summer, while 3-nitrosalicylic acid was only observed in winter, which could be attributed to their different sources, as discussed above.

The seasonal contributions of individual NACs to total light absorption of NACs at wavelength of 365 nm are shown in Fig. 3b. The relative contribution trends of 4-nitrophenol > 4-nitrocatechol > 2-methyl-4-nitrophenol > 5-nitrosalicylic acid > 3-methyl-4-nitrophenol, 4-nitrophenol > 4-nitrocatechol > 5-nitrosalicylic acid > 2-methyl-4-nitrophenol > 3-methyl-4-nitrophenol, 4-nitrocatechol > 4-nitrophenol > 4-methyl-5-nitrocatechol >3-methyl-5-nitrocatechol > 5-nitrosalicylic acid > 2-methyl-4-nitrophenol > 3-methyl-4-nitrophenol, and 4-nitrocatechol > 4-methyl-5-nitrocatechol > 4-nitrophenol > 3-methyl-5-nitrocatechol > 2-methyl-4-nitrophenol > 4-nitro-1-naphthol > 5-nitrosalicylic acid > 3-methyl-4-nitrophenol > 3-nitrosalicylic acid > 2,6-dimethyl-4-nitrophenol were observed in spring, summer, fall and winter, respectively. These trends are different from their concentration fractions in OC, which may be mainly due to the differences in light absorption ability (see Fig. S3). For example, 4-nitrocatechol has lower mass concentration, but higher light absorption contribution, compared to 4-nitrophenol. These results suggest that mere compositional information of NACs might not be directly translated into impacts on optical property, because they have startlingly different absorption properties.

4 Conclusions

In this study, ten individual NAC species were quantified, together with 19 organic markers, in $PM_{2.5}$ in Xi'an, Northwest China. The average concentrations of the NACs were 2.1, 1.1, 12.9, and 56 ng m^{-3} in spring, summer, fall, and winter, respectively. Higher concentrations of NACs in winter than in summer were also observed in previous studies in Asia, Europe and the USA. Four major sources of NACs were identified in Xi'an based on PMF analysis, including vehicle emission, coal combustion, secondary formation and biomass burning. On average, in spring, vehicular emission (41%) was the main contributor of NACs, and secondary formation (26%) and biomass burning (20%) also had relatively large contributions. In summer, secondary formation contributed the most (45%), which was likely due to the enhanced photochemical formation of secondary NACs that outweights photo-degradation/bleaching. Besides, vehicular emission (34%) also had a significant contribution in summer. In fall, biomass burning (45%) contributed the most, and secondary

formation (30%) and vehicular emission (23%) also made significant contributions. In winter, coal burning (39%) and biomass burning (36%) contributed the most, which can be attributed to emissions from residential heating activities. Backward trajectory cluster analyses indicate that both regional and local contributions for NACs were significant in Xi'an. Local contributions were 53, 47, 66 and 44% in the four seasons, and regional transport was mainly through the northwest transport channel. The light absorption contributions of NACs to BrC were quantified and also showed large seasonal variations. The seasonal average contributions of total NACs to BrC light absorption at wavelength of 365 nm ranged from 0.1% to 0.9%, which were 6-9 times higher than their carbon mass fractions in total OC. Our results suggest that even a small amount of chromophores can have significant impacts on the optical characteristics of BrC. More studies are needed to better understand the seasonal differences in chemical composition and formation processes of NACs and the link with their optical properties.

Data availability. Raw data used in this study are archived at the Institute of Earth Environment, Chinese Academy of Sciences, and are available on request by contacting the corresponding author.

Supplement. The Supplement related to this article is available online at

Author contributions. RJH designed the study. Data analysis was done by WY, LY, and RJH. WY, LY and RJH interpreted data, prepared the display items and wrote the manuscript. All authors commented on and discussed the manuscript.

Competing interests. The authors declare that they have no conflict of interest.

Acknowledgements. This work was supported by the National Natural Science Foundation of China (NSFC) under Grant No. 41877408, 41925015, 91644219, and 41675120, the Chinese Academy of Sciences (no. ZDBS-LY-DQC001, XDB40030202), the National Key Research and Development Program of China (No. 2017YFC0212701), and the Cross

Innovative Team fund from the State Key Laboratory of Loess and Quaternary Geology (No. SKLLQGTD1801). Yongjie Li would like to acknowledge financial support from the Multi-Year Research grant (MYRG2017-00044-FST and MYRG2018-00006-FST) from the University of Macau.

References

Al-Naiema, I. M. and Stone, E. A.: Evaluation of anthropogenic secondary organic aerosol tracers from aromatic hydrocarbons, Atmos. Chem. Phys., 17, 2053–2065, 2017.

Andreozzi, R., Canterino, M., Caprio, V., Di Somma, I., and Sanchirico, R.: Salicylic acid nitration by means of nitric acid/acetic acid system: chemical and kinetic characterization, Org. Process. Res. Dev., 10, 1199–1204, 2006.

Barsotti, F., Bartels-Rausch, T., De Laurentiis, E., Ammann, M., Brigante, M., Mailhot, G., Maurino, V., Minero, C., and Vione, D.: Photochemical formation of nitrite and nitrous acid (HONO) upon irradiation of nitrophenols in aqueous solution and in viscous secondary organic aerosol proxy, Environ. Sci. Technol., 51, 7486–7495, 2017.

Canonaco, F., Crippa, M., Slowik, J. G., Baltensperger, U., and Prévôt, A. S. H.: SoFi, an IGOR-based interface for the efficient use of the generalized multilinear engine (ME-2) for the source apportionment: ME-2 application to aerosol mass spectrometer data, Atmos. Meas. Tech., 6, 3649–3661, 2013.

Cecinato, A., Di Palo, V., Pomata, D., Tomasi Sciano, M. C., and Possanzini, M.: Measurement of phase-distributed nitrophenols in Rome ambient air, Chemosphere, 59, 679–683, doi:10.1016/j.chemosphere.2004.10.045, 2005.

Chow, J. C., Watson, J. G., Robles, J., Wang, X. L., Chen, L. W. A., Trimble, D. L., Kohl, S. D., Tropp, R. J., and Fung, K. K.: Quality assurance and quality control for thermal/optical analysis of aerosol samples for organic and elemental carbon, Anal. Bioanal. Chem., 401, 3141− 3152, 2011.

Chow, K. S., Huang, X. H. H., and Yu, J. Z.: Quantification of nitroaromatic compounds in atmospheric fine particulate matter in Hong Kong over 3 years: field measurement

evidence for secondary formation derived from biomass burning emissions, Environ. Chem., 13, 665–673, doi:10.1071/EN15174, 2015.

Delhomme, O., Morville, S., and Millet, M.: Seasonal and diurnal variations of atmospheric concentrations of phenols and nitrophenols measured in the Strasbourg area, France, Atmos. Pollut. Res., 1, 16–22, doi:10.5094/APR.2010.003, 2010.

Desyaterik, Y., Sun, Y., Shen, X., Lee, T., Wang, X., Wang, T., and Collett, J. L.: Speciation of "brown" carbon in cloud water impacted by agricultural biomass burning in eastern China, J. Geophys. Res.-Atmos., 118, 7389–7399, https://doi.org/10.1002/jgrd.50561, 2013.

Feng, Y., Ramanathan, V., and Kotamarthi, V. R.: Brown carbon: a significant atmospheric absorber of solar radiation?, Atmos. Chem. Phys., 13, 8607−8621, 2013.

Finewax, Z., de Gouw, J. A., and Ziemann, P. J.: Identification and quantification of 4-nitrocatechol formed from OH and NO_3 radical-initiated reactions of catechol in air in the presence of NOx: implications for secondary organic aerosol formation from biomass burning, Environ. Sci. Technol., 52, 1981–1989, 2018.

Harrison, M. A. J., Barra, S., Borghesi, D., Vione, D., Arsene, C., and Olariu, R. I.: Nitrated phenols in the atmosphere: a review, Atmos. Environ., 39, 231−248, 2005.

Hecobian, A., Zhang, X., Zheng, M., Frank, N. H., Edgerton, E. S., and Weber, R. J.: Water-soluble organic aerosol material and the light absorption characteristics of aqueous extracts measured over the Southeastern United States, Atmos. Chem. Phys., 10, 5965−5977, 2010.

Hems, R. F. and Abbatt, J. P. D.: Aqueous phase photo-oxidation of brown carbon nitrophenols: reaction kinetics, mechanism, and evolution of light absorption, ACS Earth Space Chem., 2, 225-234, 2018.

Hinkel, M., Reischl, A., Schramm, K.-W., Trautner, F., Reissinger, M., and Hutzinger, O.: Concentration levels of nitrated phenols in conifer needles, Chemosphere, 18, 2433–2439, 1989.

Hoffmann, D., Iinuma, Y., and Herrmann, H.: Development of a method for fast analysis of phenolic molecular markers in biomass burning particles using high performance liquid

chromatography/atmospheric pressure chemical ionisation mass spectrometry, J. Chromatogr. A, 1143, 168–175, doi:10.1016/j.chroma.2007.01.035, 2007.

Iinuma, Y., Böge, O., Gräfe, R., and Herrmann, H.: Methyl-nitrocatechols: atmospheric tracer compounds for biomass burning secondary organic aerosols, Environ. Sci. Technol., 44, 8453–8459, doi:10.1021/Es102938a, 2010.

Ikemori, F., Nakayama, T., and Hasegawa, H.: Characterization and possible sources of nitrated mono- and di-aromatic hydrocarbons containing hydroxyl and/or carboxyl functional groups in ambient particles in Nagoya, Japan, Atmos. Environ., 211, 91-102, 2019.

Inomata, S., Tanimoto, H., Fujitani, Y., Sekimoto, K., Sato, K., Fushimi, A., Yamada, H., Hori, S., Kumazawa, Y., Shimono, A., and Hikida, T.: On-line measurements of gaseous nitro-organic compounds in diesel vehicle exhaust by proton-transfer-reaction mass spectrometry, Atmos. Environ., 73, 195–203, doi:10.1016/j.atmosenv.2013.03.035, 2013.

Jang, M. and Kamens, R. M.: Characterization of secondary aerosol from the photooxidation of toluene in the presence of NOx and 1-propene, Environ. Sci. Technol., 35, 3626–3639, 2001.

Ju, K.-S. and Parales, R. E.: Nitroaromatic compounds, from synthesis to biodegradation, Microbiol. Mol. Biol. Rev., 74, 250-272, 2010.

Kahnt, A., Behrouzi, S., Vermeylen, R., Safi Shalamzari, M., Vercauteren, J., Roekens, E., Claeys, M., and Maenhaut, W.: One-year study of nitro-organic compounds and their relation to wood burning in PM_{10} aerosol from a rural site in Belgium, Atmos. Environ., 81, 561–568, https://doi.org/10.1016/j.atmosenv.2013.09.041, 2013.

Kitanovski, Z., Grgic, I., Vermeylen, R., Claeys, M., and Maenhaut, W.: Liquid chromatography tandem mass spectrometry method for characterization of monoaromatic nitro-compounds in atmospheric particulate matter, J. Chromatogr. A, 1268, 35–43, doi:10.1016/j.chroma.2012.10.021, 2012.

Kitanovski, Z., Cusak, A., Grgic´, I., and Claeys, M.: Chemical characterization of the main products formed through aqueous-phase photonitration of guaiacol, Atmos. Meas. Tech., 7, 2457–2470, https://doi.org/10.5194/amt-7-2457-2014, 2014.

Kovacic, P. and Somanathan, R.: Nitroaromatic compounds: environmental toxicity, carcinogenicity, mutagenicity, therapy and mechanism, J. Appl. Toxicol., 34, 810-824, 2014.

Laskin, A., Laskin, J., and Nizkorodov, S. A.: Chemistry of atmospheric brown carbon, Chem. Rev., 115, 4335−4382, 2015.

Li, M., Wang, X., Lu, C., Li, R., Zhang, J., Dong, S., Yang, L., Xue, L., Chen, J., and Wang, W.: Nitrated phenols and the phenolic precursors in the atmosphere in urban Jinan, China, Sci. Total Environ., 714, 136760, 2020.

Li, X., Yang, Y., Liu, S., Zhao, Q., Wang, G., and Wang, Y.: Light absorption properties of brown carbon (BrC) in autumn and winter in Beijing: composition, formation and contribution of nitrated aromatic compounds, Atmos. Environ., 223, 117289, 2020.

Lin, P., Liu, J. M., Shilling, J. E., Kathmann, S. M., Laskin, J., and Laskin, A.: Molecular characterization of brown carbon (BrC) chromophores in secondary organic aerosol generated from photo-oxidation of toluene, Phys. Chem. Chem. Phys., 17, 23312–23325, doi:10.1039/C5CP02563J, 2015.

Lin, P., Aiona, P. K., Li, Y., Shiraiwa, M., Laskin, J., Nizkorodov, S. A., and Laskin, A.: Molecular characterization of brown carbon in biomass burning aerosol particles, Environ. Sci. Technol., 50, 11815-11824, 2016.

Lin, P., Fleming, L. T., Nizkorodov, S. A., Laskin, J., and Laskin, A.: Comprehensive molecular characterization of atmospheric brown carbon by high resolution mass spectrometry with electrospray and atmospheric pressure photoionization, Anal. Chem., 90, 12493–12502, 2018.

Lu, C., Wang, X., Li, R., Gu, R., Zhang, Y., Li, W., Gao, R., Chen, B., Xue, L., and Wang, W.: Emissions of fine particulate nitrated phenols from residential coal combustion in China, Atmos. Environ., 203, 10–17, https://doi.org/10.1016/j.atmosenv.2019.01.047, 2019a.

Lu, C., Wang, X., Dong, S., Zhang, J., Li, J., Zhao, Y., Liang, Y., Xue, L., Xie, H., Zhang, Q., and Wang, W.: Emissions of fine particulate nitrated phenols from various on-road vehicles in China, Environ. Res., 179, 108709, https://doi.org/10.1016/j.envres.2019.108709, 2019b.

513 Ma, Y., Cheng, Y., Qiu, X., Cao, G., Fang, Y., Wang, J., Zhu, T., and Hu, D.: Sources and
514 oxidative potential of water-soluble humic-like substances ($HULIS_{WS}$) in fine particulate
515 matter ($PM_{2.5}$) in Beijing, Atmos. Chem. Phys., 18, 5607-5617, 2018.
516 Ma, Y., Cheng, Y., Qiu, X., Cao, G., Kuang, B., Yu, J. Z., and Hu, D.: Optical properties,
517 source apportionment and redox activity of humic-like substances (HULIS) in airborne
518 fine particulates in Hong Kong, Environ. Pollut., 255, 113087, 2019.
519 Mohr, C., Lopez-Hilfiker, F. D., Zotter, P., Prévôt, A. S., Xu, L., Ng, N. L., Herndon, S. C.,
520 Williams, L. R., Franklin, J. P., Zahniser, M. S., Worsnop, D. R., Knighton, W. B., Aiken,
521 A. C., Gorkowski, K. J., Dubey, M. K., Allan, J. D., and Thornton, J. A.: Contribution of
522 nitrated phenols to wood burning brown carbon light absorption in Detling, United
523 Kingdom during winter time, Environ. Sci. Technol., 47, 6316–6324,
524 https://doi.org/10.1021/es400683v, 2013.
525 Natangelo, M., Mangiapan, S., Bagnati, R., Benfenati, E., and Fanelli, R.: Increased
526 concentrations of nitrophenols in leaves from a damaged forestal site, Chemosphere, 38,
527 1495–1503, doi:10.1016/S0045-6535(98)00370-1, 1999.
528 Olson, M. R., Garcia, M. V., Robinson, M. A., Van Rooy, P., Dietenberger, M. A., Bergin, M.,
529 and Schauer, J. J.: Investigation of black and brown carbon multiple-wavelength
530 dependent light absorption from biomass and fossil fuel combustion source emissions, J.
531 Geophys. Res., 120, 6682–6697, doi:10.1002/2014JD022970, 2015.
532 Paatero, P.: Least squares formulation of robust non-negative factor analysis, Chemometr.
533 Intell. Lab., 37, 23–35, 1997.
534 Perrone, M. G., Carbone, C., Faedo, D., Ferrero, L., Maggioni, A., Sangiorgi, G., and
535 Bolzacchini, E.: Exhaust emissions of polycyclic aromatic hydrocarbons, n-alkanes and
536 phenols from vehicles coming within different European classes, Atmos. Environ., 82,
537 391–400, 2014.
538 Purohit, V. and Basu, A. K.: Mutagenicity of nitroaromatic compounds, Chem. Res. Toxicol.,
539 13, 673–692, 2000.
540 Richartz, H., Reischl, A., Trautner, F., and Hutzinger, O.: Nitrated phenols in fog, Atmos.
541 Environ., 24A, 3067-3071, https://doi.org/10.1016/0960-1686(90)90485-6, 1990.

Schummer, C., Groff, C., Chami, J. A., Jaber, F., and Millet, M.: Analysis of phenols and nitrophenols in rainwater collected simultaneously on an urban and rural site in east of France, Sci. Total Environ., 407, 5637-5643, https://doi.org/10.1016/j.scitotenv.2009.06.051, 2009.

Taneda, S., Mori, Y., Kamata, K., Hayashi, H., Furuta, C., Li, C., Seki, K., Sakushima, A., Yoshino, S., Yamaki, K., Watanabe, G., Taya, K., and Suzuki, A. K.: Estrogenic and anti-androgenic activity of nitrophenols in diesel exhaust particles (DEP), Biol. Pharm. Bull., 27, 835–837, 2004.

Teich, M., van Pinxteren, D., Wang, M., Kecorius, S., Wang, Z., Müller, T., Mocnik, G., and Herrmann, H.: Contributions of nitrated aromatic compounds to the light absorption of water-soluble and particulate brown carbon in different atmospheric environments in Germany and China, Atmos. Chem. Phys., 17, 1653–1672, https://doi.org/10.5194/acp-17-1653-2017, 2017.

Tremp, J., Mattrel, P., Fingler, S., and Giger, W.: Phenols and nitrophenols as tropospheric pollutants: emissions from automobile exhausts and phase transfer in the atmosphere, Water Air Soil Poll., 68, 113–123, https://doi.org/10.1007/bf00479396, 1993.

Vanni, A., Pellegrino, V., Gamberini, R., and Calabria, A.: An evidence for nitrophenol contamination in Antarctic fresh-water and snow. Simultaneous determination of nitrophenols and nitroarenes at ng/L levels, Int. J. Environ. Anal. Chem., 79, 349-365, http:// doi.org/10.1080/03067310108044394, 2001.

Vione, D., Maurino, V., Minero, C., and Pelizzetti, E.: Phenol photonitration upon UV irradiation of nitrite in aqueous solution I: effects of oxygen and 2-propanol, Chemosphere, 45, 893–902, https://doi.org/10.1016/s0045-6535(01)00035-2, 2001.

Vione, D., Maurino, V., Minero, C., and Pelizzetti, E.: Aqueous atmospheric chemistry: formation of 2,4-dinitrophenol upon nitration of 2-nitrophenol and 4-nitrophenol in solution, Environ. Sci. Technol., 39, 7921–7931, doi:10.1021/es050824m, 2005.

Wang, G. H., Kawamura, K., Lee, S., Ho, K. F., and Cao, J. J.: Molecular, seasonal, and spatial distributions of organic aerosols from fourteen Chinese cities, Environ. Sci. Technol., 40, 4619-4625, https://doi.org/10.1021/es060291x, 2006.

Wang, L. W., Wang, X. F., Gu, R. R., Wang, H., Yao, L., Wen, L., Zhu, F. P., Wang, W. H., Xue, L. K., Yang, L. X., Lu, K. D., Chen, J. M., Wang, T., Zhang, Y. H., and Wang, W. X.: Observations of fine particulate nitrated phenols in four sites in northern China: concentrations, source apportionment, and secondary formation, Atmos. Chem. Phys., 18, 4349-4359, 2018.

Wang, X., Gu, R., Wang, L., Xu, W., Zhang, Y., Chen, B., Li, W., Xue, L., Chen, J., and Wang, W.: Emissions of fine particulate nitrated phenols from the burning of five common types of biomass, Environ. Pollut., 230, 405–412, https://doi.org/10.1016/j.envpol.2017.06.072, 2017.

Wang, Y., Hu, M., Wang, Y., Zheng, J., Shang, D., Yang, Y., Liu, Y., Li, X., Tang, R., and Zhu, W.: The formation of nitro-aromatic compounds under high NOx and anthropogenic VOC conditions in urban Beijing, China, Atmos. Chem. Phys., 19, 7649–7665, https://doi.org/10.5194/acp-19-7649-2019, 2019.

Wang, Y. Q., Zhang, X. Y., and Draxler, R.: TrajStat: GIS-based software that uses various trajectory statistical analysis methods to identify potential sources from long-term air pollution measurement data, Environ. Modell. Softw., 24, 938-939, 2009.

Wojcik, G. S. and Chang, J. S.: A re-evaluation of sulfur budgets, lifetimes, and scavenging ratios for eastern north America, J. Atmos. Chem., 26, 109-145, 1997.

Xie, M. J., Chen, X., Hays, M. D., Lewandowski, M., Offenberg, J., Kleindienst, T. E., and Holder, A. L.: Light absorption of secondary organic aerosol: composition and contribution of nitroaromatic compounds, Environ. Sci. Technol., 51, 11607−11616, 2017.

Xie, M. J., Chen, X., Holder, A. L., Hays, M. D., Lewandowski, M., Offenberg, J. H., Kleindienst, T. E., Jaoui, M., and Hannigan, M. P.: Light absorption of organic carbon and its sources at a southeastern U.S. location in summer, Environ. Pollut., 244, 38–46, https://doi.org/10.1016/j.envpol.2018.09.125, 2019.

Yuan, B., Liggio, J., Wentzell, J., Li, S.-M., Stark, H., Roberts, J. M., Gilman, J., Lerner, B., Warneke, C., Li, R., Leithead, A., Osthoff, H. D., Wild, R., Brown, S. S., and de Gouw, J. A.: Secondary formation of nitrated phenols: insights from observations during the

Uintah Basin Winter Ozone Study (UBWOS) 2014, Atmos. Chem. Phys., 16, 2139–2153, https://doi.org/10.5194/acp-16-2139-2016, 2016.

Yuan, W., Huang, R. J., Yang, L., Guo, J., Chen, Z. Y., Duan, J., Wang, T., Ni, H. Y., Han, Y. M., Li, Y. J., Chen, Q., Chen, Y., Hoffmann, T., and O'Dowd, C.: Characterization of the light-absorbing properties, chromophore composition and sources of brown carbon aerosol in Xi'an, northwestern China, Atmos. Chem. Phys., 20, 5129-5144, 2020.

Zhang, X. L., Lin, Y. H., Surratt, J. D., and Weber, R. J.: Sources, composition and absorption angstrom exponent of light-absorbing organic components in aerosol extracts from the Los Angeles Basin, Environ. Sci. Technol., 47, 3685–3693, doi:10.1021/es305047b, 2013.

Zhang, Y., Forrister, H., Liu, J., Dibb, J., Anderson, B., Schwarz, J. P., Perring, A. E., Jimenez, J. L., Campuzano-Jost, P., Wang, Y., Nenes, A., and Weber, R. J.: Top-of-atmosphere radiative forcing affected by brown carbon in the upper troposphere, Nat. Geosci., 10, 486–489, https://doi.org/10.1038/ngeo2960, 2017.

615 **Table 1.** Mean and standard deviation (if applicable) of the measured mass concentrations of

616 individual NACs in Xi'an in comparison to those in other studies.

Locations	Concentrations (ng m^{-3})										Reference
	4NP	2M4NP	3M4NP	2,6DM4NP	4N1N	4NC	3M5NC	4M5NC	3NSA	5NSA	
Europe											
TROPOS, Germany, winter 2014	7.09	3.64	2.60	0.65					1.36	0.94	Teich et al., 2017
	(7.08)	(3.05)	(2.22)	(0.58)					(1.02)	(0.75)	
Melpitz, Germany, summer 2014	0.06	0.04	0.03						0.17	0.09	Teich et al., 2017
	(0.03)	(0.00)	(0.00)						(0.15)	(0.09)	
Melpitz, Germany, winter 2014	4.09	3.64	2.44	0.91					0.66	0.32	Teich et al., 2017
	(3.27)	(3.06)	(2.20)	(0.90)					(0.69)	(0.24)	
Ljubljana, Slovenia, summer 2010	0.15	0.05	<0.03			0.24	0.1	0.06	0.09	0.18	Kitanovski et al., 2012
Ljubljana, Slovenia, winter 2010	1.8	0.75	0.61			75	34	29	1.3	1.4	Kitanovski et al., 2012
Villa Ada park, Rome, spring 2003	17.8		7.8	5.9							Cecinato et al., 2005
	(5.6)		(2.6)	(2.9)							
Waldstein, Germany, summer 2014									0.17	0.23	Teich et al., 2017
									(0.11)	(0.12)	
USA											
Research Triangle Park, USA, summer	0.018	0.005				0.057					Xie et al., 2019
2013	(0.027)	(0.009)				(0.042)					
Lowa City, USA, fall 2015	0.63	0.08				1.60		1.61		0.14	Al-Naiema and Stone,
	(0.48)	(0.05)				(2.88)		(1.77)		(0.08)	2017
Asia											
Hong Kong, China, spring 2012	0.36	0.18	0.03	0.01		0.25	0.05	0.05			Chow et al., 2015
Hong Kong, China, summer 2012	0.54	0.3	0.02	0.01		1.48	0.63	0.25			Chow et al., 2015
Hong Kong, China, fall 2012	0.92	0.39	0.04	0.01		2.45	0.94	0.44			Chow et al., 2015
Hong Kong, China, winter 2012	1.13	0.65	0.07	0.01		2.39	1.35	0.53			Chow et al., 2015
Xianghe, China, summer 2013	0.98	0.32	0.09	0.06					1.21	0.88	Teich et al., 2017
	(0.78)	(0.21)	(0.07)	(0.05)					(1.45)	(0.64)	
Wangdu, China, summer 2014	2.63	0.68	0.21	0.06					3.14	1.63	Teich et al., 2017
	(2.66)	(0.78)	(0.35)	(0.09)					(3.05)	(0.78)	
Xi'an, China, spring 2016	1.19	0.24	0.18			0.28				0.15	This study
	(0.36)	(0.08)	(0.05)			(0.18)				(0.15)	
Xi'an, China, summer 2016	0.45	0.10	0.07			0.16				0.29	This study
	(0.28)	(0.10)	(0.06)			(0.11)				(0.41)	
Xi'an, China, fall 2016	3.6	0.73	0.44			3.9	1.23	1.35		1.72	This study
	(2.6)	(0.54)	(0.35)			(4.0)	(1.34)	(1.24)		(2.3)	
Xi'an, China, winter 2015	15.6	4.5	3.4	0.55	1.16	15.5	6.4	6.2	0.84	2.3	This study
	(6.6)	(1.72)	(1.52)	(0.39)	(0.53)	(7.4)	(3.7)	(2.9)	(0.56)	(2.4)	
Nagoya, summer 2013	1.1	0.49	0.17		0.98	0.74		0.081	0.33	0.75	Ikemori et al., 2019
	(0.54)	(0.48)	(0.13)		(1.5)	(0.72)		(0.077)	(0.38)	(0.84)	
Nagoya, Japan, fall 2013	7.0	3.2	1.1		0.76	6.8		1.6	0.27	0.67	Ikemori et al., 2019
	(3.9)	(2.7)	(0.76)		(0.64)	(10.8)		(2.9)	(0.20)	(0.41)	

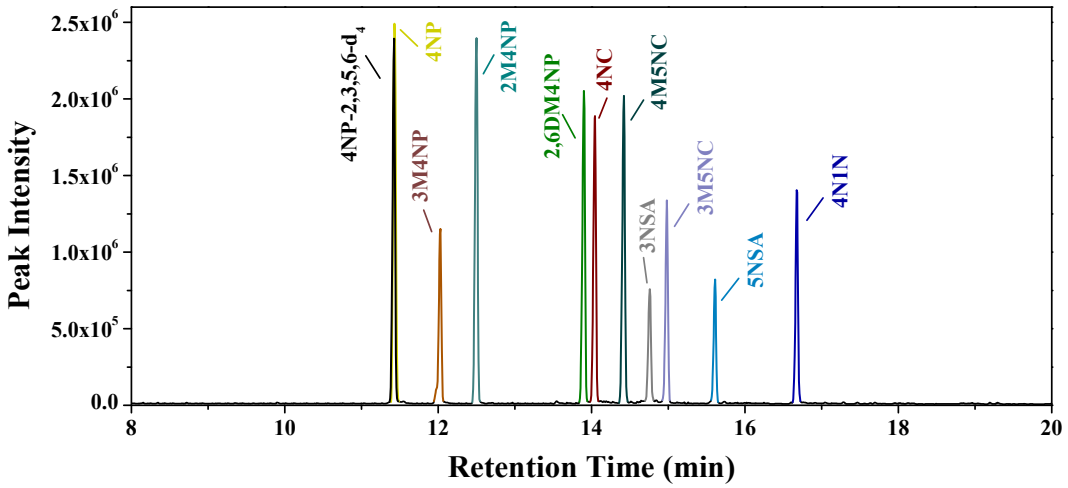

617

618 **Figure 1.** Selected ion monitoring chromatograms for the nitrated aromatic compound

619 standards (2 ug mL^{-1}). (4NP-2,3,5,6-d_4: 4-nitrophenol-2,3,5,6-d_4, 4NP: 4-nitrophenol, 3M4NP:

620 3-methyl-4-nitrophenol, 2M4NP: 2-methyl-4-nitrophenol, 2,6DM4NP:

621 2,6-dimethyl-4-nitrophenol, 4NC: 4-nitrocatechol, 4M5NC: 4-methyl-5-nitrocatechol, 3NSA:

622 3-nitrosalicylic acid, 3M5NC: 3-methyl-5-nitrocatechol, 5NSA: 5-nitrosalicylic acid, 4N1N:

623 4-nitro-1-naphthol).

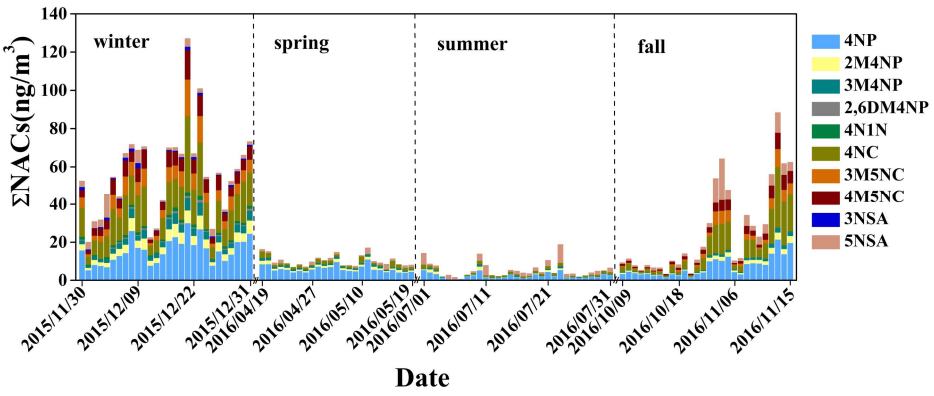

Figure 2. Time series of the concentrations of nitrated aromatic compounds in the aerosol sample (spring and summer × 5, fall ×2). The full names of the compounds are given in Table S1.

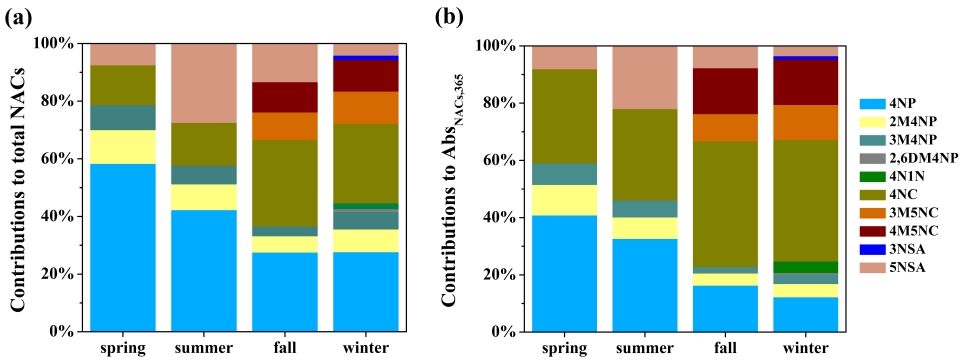

628

629 **Figure 3.** Average contributions of individual nitrated aromatic compounds to (a) the total
630 concentration and (b) the total light absorption at wavelength 365 nm of particulate nitrated
631 aromatic compounds in four seasons. The full names of the compounds are given in Table S1.

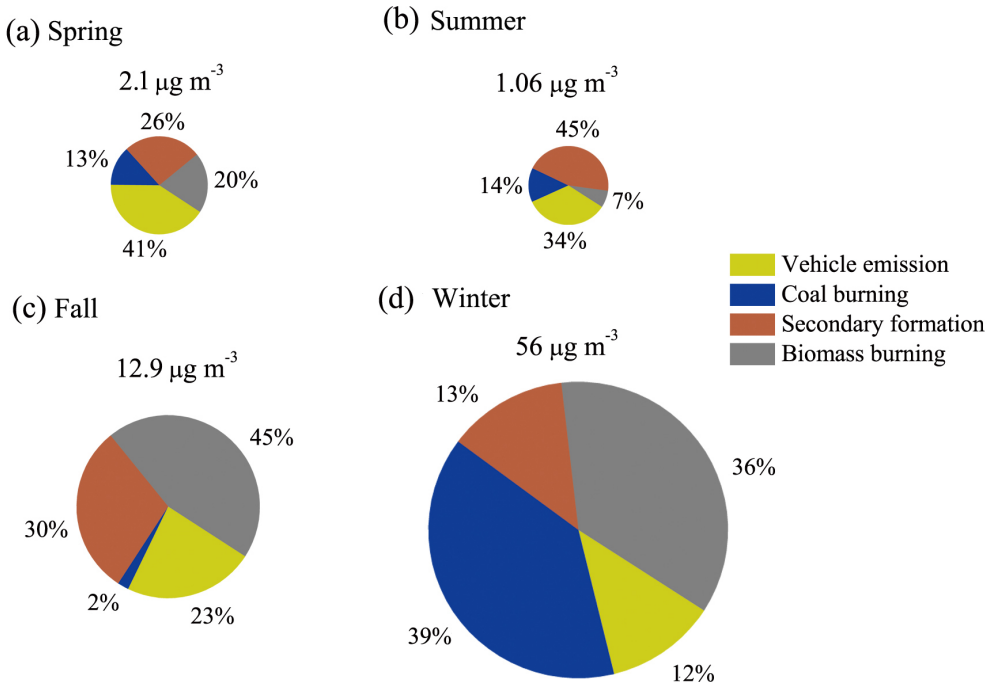

632 **Figure 4.** Contributions of source factors to the concentrations of NACs in four seasons.

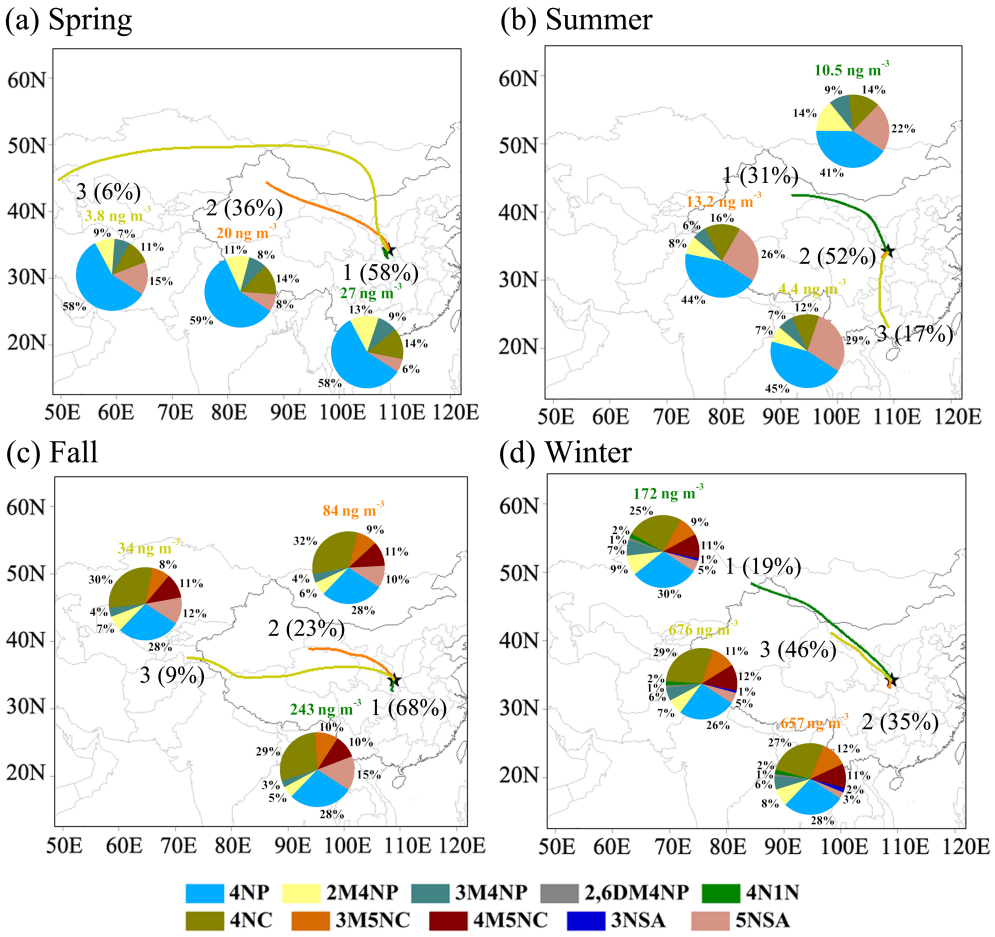

633 **Figure 5.** NACs at each 72-h backward trajectory cluster during (a) spring, (b) summer, (c)

634 fall and (d) winter. The full names of the compounds are given in Table S1.

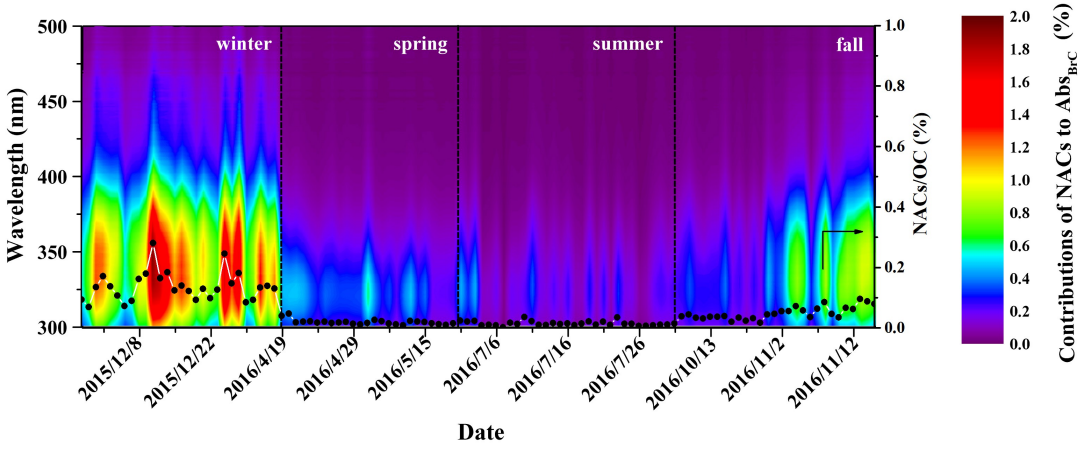

Figure 6. Time series of the light absorption contributions of total NACs to Abs of brown carbon over the wavelength from 300 to 500 nm (color scale and left axis), and the ratio of concentration of NACs to organic carbon (dots and right axis).

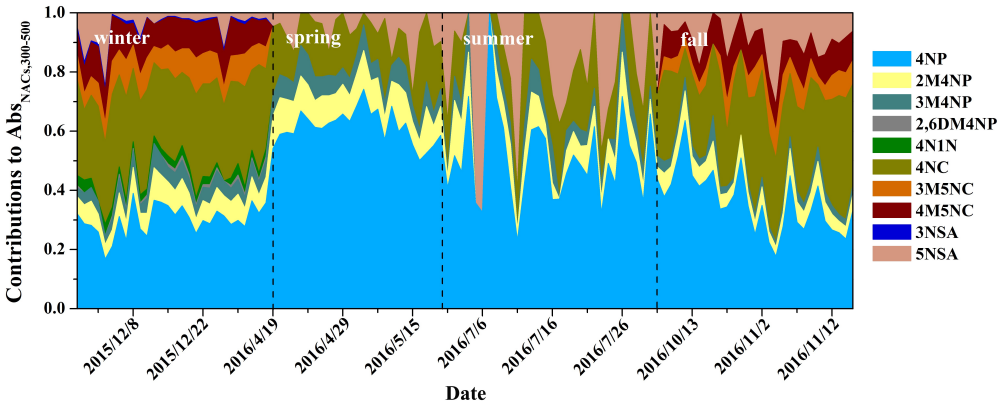

636

637 **Figure 7.** Daily contributions of individual NACs to light absorption of total NACs at

638 wavelength of 300-500 nm. The full names of the compounds are given in Table S1.